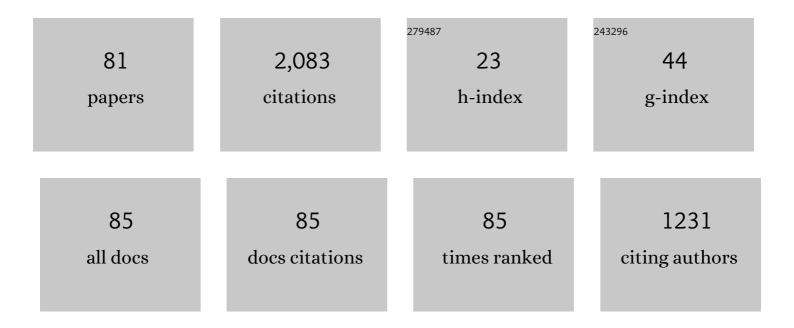
Janghoon Seo

List of Publications by Year in descending order

Source: https://exaly.com/author-pdf/2358235/publications.pdf Version: 2024-02-01



IANCHOON SEO

#	Article	IF	CITATIONS
1	Development of a gyrokinetic hyperbolic solver based on discontinuous Galerkin method in tokamak geometry. Computer Physics Communications, 2022, 273, 108265.	3.0	3
2	Toward the core-edge coupling of delta-f and total-f gyrokinetic models. Physics of Plasmas, 2022, 29, 032301.	0.7	1
3	Effects of light impurities on zonal flow activities and turbulent thermal transport. Physics of Plasmas, 2022, 29, .	0.7	6
4	Nonlinear Fokker-Planck collision operator in Rosenbluth form for gyrokinetic simulations using discontinuous Galerkin method. Computer Physics Communications, 2022, 279, 108459.	3.0	0
5	A new hybrid simulation model for tokamak plasma turbulence. Computer Physics Communications, 2021, 258, 107626.	3.0	2
6	First coupled GENE–XGC microturbulence simulations. Physics of Plasmas, 2021, 28, 012303.	0.7	9
7	Constructing a new predictive scaling formula for ITER's divertor heat-load width informed by a simulation-anchored machine learning. Physics of Plasmas, 2021, 28, .	0.7	22
8	Spatial coupling of gyrokinetic simulations, a generalized scheme based on first-principles. Physics of Plasmas, 2021, 28, .	0.7	12
9	A Framework for International Collaboration on ITER Using Large-Scale Data Transfer to Enable Near-Real-Time Analysis. Fusion Science and Technology, 2021, 77, 98-108.	0.6	2
10	Tokamak ITG-KBM transition benchmarking with the mixed variables/pullback transformation electromagnetic gyrokinetic scheme. Physics of Plasmas, 2021, 28, 034501.	0.7	6
11	Encoder–decoder neural network for solving the nonlinear Fokker–Planck–Landau collision operator in XGC. Journal of Plasma Physics, 2021, 87, .	0.7	9
12	Property of neoclassical GAMs induced by pellet generated plasma perturbations in the gyrokinetic code XGC. Physics of Plasmas, 2021, 28, 044501.	0.7	0
13	Implementation of higher-order velocity mapping between marker particles and grid in the particle-in-cell code XGC. Journal of Plasma Physics, 2021, 87, .	0.7	3
14	Improving Gyrokinetic Field Solvers toward Whole-Volume Modeling of Stellarators. Plasma and Fusion Research, 2021, 16, 2403054-2403054.	0.3	1
15	Verification of a fully implicit particle-in-cell method for the v â^¥-formalism of electromagnetic gyrokinetics in the XGC code. Physics of Plasmas, 2021, 28, 072505.	0.7	7
16	Advancing Fusion with Machine Learning Research Needs Workshop Report. Journal of Fusion Energy, 2020, 39, 123-155.	0.5	17
17	Comparison of edge turbulence characteristics between DIII-D and C-Mod simulations with XGC1. Physics of Plasmas, 2020, 27, .	0.7	4
18	Reduction of blob-filament radial propagation by parallel variation of flows: Analysis of a gyrokinetic simulation. Physics of Plasmas, 2020, 27, .	0.7	5

Janghoon Seo

#	Article	IF	CITATIONS
19	Finding Structure in Large Data Sets of Particle Distribution Functions Using Unsupervised Machine Learning. IEEE Transactions on Plasma Science, 2020, , 1-4.	0.6	Ο
20	Nonlinear global gyrokinetic delta- <i>f</i> turbulence simulations in a quasi-axisymmetric stellarator. Physics of Plasmas, 2020, 27, .	0.7	12
21	Gyrokinetic understanding of the edge pedestal transport driven by resonant magnetic perturbations in a realistic divertor geometry. Physics of Plasmas, 2020, 27, .	0.7	15
22	Verification of an improved equation-free projective integration method for neoclassical plasma-profile evolution in tokamak geometry. Physics of Plasmas, 2020, 27, 032505.	0.7	2
23	Spatial core-edge coupling of the particle-in-cell gyrokinetic codes GEM and XGC. Physics of Plasmas, 2020, 27, 122510.	0.7	10
24	Study of up–down poloidal density asymmetry of high- impurities with the new impurity version of XGCa. Journal of Plasma Physics, 2019, 85, .	0.7	10
25	Verification of the global gyrokinetic stellarator code XGC-S for linear ion temperature gradient driven modes. Physics of Plasmas, 2019, 26, .	0.7	15
26	Development of a Gyrokinetic Particle-in-Cell Code for Whole-Volume Modeling of Stellarators. Plasma, 2019, 2, 179-200.	0.7	11
27	X-point ion orbit physics in scrape-off layer and generation of a localized electrostatic potential perturbation around X-point. Physics of Plasmas, 2019, 26, 014504.	0.7	3
28	Comparative collisionless alpha particle confinement in stellarator reactors with the XGC gyrokinetic code. Physics of Plasmas, 2019, 26, 032506.	0.7	11
29	A Co-Design Study Of Fusion Whole Device Modeling Using Code Coupling. , 2019, , .		2
30	Cross-verification of neoclassical transport solutions from XGCa against NEO. Physics of Plasmas, 2019, 26, .	0.7	7
31	A fast low-to-high confinement mode bifurcation dynamics in the boundary-plasma gyrokinetic code XGC1. Physics of Plasmas, 2018, 25, .	0.7	79
32	In Situ Analysis and Visualization of Fusion Simulations: Lessons Learned. Lecture Notes in Computer Science, 2018, , 230-242.	1.0	2
33	Gyroaveraging operations using adaptive matrix operators. Physics of Plasmas, 2018, 25, .	0.7	7
34	A tight-coupling scheme sharing minimum information across a spatial interface between gyrokinetic turbulence codes. Physics of Plasmas, 2018, 25, 072308.	0.7	17
35	Analysis of equilibrium and turbulent fluxes across the separatrix in a gyrokinetic simulation. Physics of Plasmas, 2018, 25, 072306.	0.7	4
36	Cross-verification of the global gyrokinetic codes GENE and XGC. Physics of Plasmas, 2018, 25, 062308.	0.7	26

JANGHOON SEO

#	Article	IF	CITATIONS
37	Gyrokinetic simulation study of magnetic island effects on neoclassical physics and micro-instabilities in a realistic KSTAR plasma. Physics of Plasmas, 2018, 25, .	0.7	24
38	What happens to full-f gyrokinetic transport and turbulence in a toroidal wedge simulation?. Physics of Plasmas, 2017, 24, .	0.7	7
39	Investigation of the plasma shaping effects on the H-mode pedestal structure using coupled kinetic neoclassical/MHD stability simulations. Physics of Plasmas, 2017, 24, .	0.7	7
40	Verification of long wavelength electromagnetic modes with a gyrokinetic-fluid hybrid model in the XGC code. Physics of Plasmas, 2017, 24, 054508.	0.7	14
41	Pedestal and edge electrostatic turbulence characteristics from an XGC1 gyrokinetic simulation. Plasma Physics and Controlled Fusion, 2017, 59, 105014.	0.9	28
42	Fast Low-to-High Confinement Mode Bifurcation Dynamics in a Tokamak Edge Plasma Gyrokinetic Simulation. Physical Review Letters, 2017, 118, 175001.	2.9	73
43	Full-f XGC1 gyrokinetic study of improved ion energy confinement from impurity stabilization of ITG turbulence. Physics of Plasmas, 2017, 24, .	0.7	14
44	Towards Real-Time Detection and Tracking of Spatio-Temporal Features: Blob-Filaments in Fusion Plasma. IEEE Transactions on Big Data, 2016, 2, 262-275.	4.4	13
45	Persistent Data Staging Services for Data Intensive In-situ Scientific Workflows. , 2016, , .		6
46	Mesh generation for confined fusion plasma simulation. Engineering With Computers, 2016, 32, 285-293.	3.5	18
47	Kinetic modeling of divertor heat load fluxes in the Alcator C-Mod and DIII-D tokamaks. Physics of Plasmas, 2015, 22, .	0.7	9
48	Exploring Data Staging Across Deep Memory Hierarchies for Coupled Data Intensive Simulation Workflows. , 2015, , .		26
49	POSTER: Leveraging deep memory hierarchies for data staging in coupled data-intensive simulation workflows. , 2014, , .		5
50	Kinetic neoclassical transport in the H-mode pedestal. Physics of Plasmas, 2014, 21, .	0.7	34
51	Intrinsic momentum generation by a combined neoclassical and turbulence mechanism in diverted DIII-D plasma edge. Physics of Plasmas, 2014, 21, 092501.	0.7	23
52	A Fokker-Planck-Landau collision equation solver on two-dimensional velocity grid and its application to particle-in-cell simulation. Physics of Plasmas, 2014, 21, .	0.7	36
53	ISABELA for effective in situ compression of scientific data. Concurrency Computation Practice and Experience, 2013, 25, 524-540.	1.4	62
54	Energy conservation tests of a coupled kinetic plasma–kinetic neutral transport code. Computational Science & Discovery, 2013, 6, 015006.	1.5	11

JANGHOON SEO

#	Article	IF	CITATIONS
55	Bootstrap current for the edge pedestal plasma in a diverted tokamak geometry. Physics of Plasmas, 2012, 19, .	0.7	31
56	Plasma transport in stochastic magnetic field caused by vacuum resonant magnetic perturbations at diverted tokamak edge. Physics of Plasmas, 2010, 17, .	0.7	76
57	Molecular dynamics simulation of hyperthermal neutrals generated by energetic ion impact on a metal plate. Journal of Applied Physics, 2010, 107, 013304.	1.1	1
58	Numerical study of the plasma wall-bias effect on the ion flux through acceleration grid hole. Physics of Plasmas, 2010, 17, 073505.	0.7	3
59	On the validity of the local diffusive paradigm in turbulent plasma transport. Physical Review E, 2010, 82, 025401.	0.8	155
60	Compressed ion temperature gradient turbulence in diverted tokamak edge. Physics of Plasmas, 2009, 16, .	0.7	80
61	Computational Knowledge for Toroidal Confinement Physics: Part I. , 2009, , .		1
62	Scaling to 150K cores: Recent algorithm and performance engineering developments enabling XGC1 to run at scale. Journal of Physics: Conference Series, 2009, 180, 012036.	0.3	21
63	Spontaneous rotation sources in a quiescent tokamak edge plasma. Physics of Plasmas, 2008, 15, .	0.7	86
64	Particle Simulation of Neoclassical Transport in the Plasma Edge. Contributions To Plasma Physics, 2006, 46, 496-503.	0.5	14
65	Wall intersection of ion orbits induced by fast transport of pedestal plasma over an electrostatic potential hill in a tokamak plasma edge. Physics of Plasmas, 2005, 12, 102501.	0.7	11
66	Property of an X-point generated velocity-space hole in a diverted tokamak plasma edge. Physics of Plasmas, 2004, 11, 5626-5633.	0.7	42
67	Numerical study of neoclassical plasma pedestal in a tokamak geometry. Physics of Plasmas, 2004, 11, 2649-2667.	0.7	158
68	X-transport: A baseline nonambipolar transport in a diverted tokamak plasma edge. Physics of Plasmas, 2002, 9, 3884-3892.	0.7	73
69	Effect of poloidal electric field on electron cyclotron current drive in a tokamak geometry. Physics of Plasmas, 2000, 7, 4948-4959.	0.7	0
70	Strong variation of average ion energy in oscillation frequency of sheath potential. Physics of Plasmas, 2000, 7, 766-769.	0.7	6
71	Feasibility experiments for electron ripple injection on current drive experiment-upgrade. Physics of Plasmas, 1998, 5, 966-972.	0.7	3
72	Deuterium–tritium plasmas in novel regimes in the Tokamak Fusion Test Reactor. Physics of Plasmas, 1997, 4, 1714-1724.	0.7	27

JANGHOON SEO

#	Article	IF	CITATIONS
73	Variational calculation of alphaâ€driven bootstrap current in a deutrium–tritium tokamak reactor. Physics of Plasmas, 1996, 3, 3732-3744.	0.7	4
74	Temperature anisotropy in a cyclotron resonance heated tokamak plasma and the generation of poloidal electric field. Physics of Plasmas, 1995, 2, 2044-2054.	0.7	29
75	Review of deuterium–tritium results from the Tokamak Fusion Test Reactor. Physics of Plasmas, 1995, 2, 2176-2188.	0.7	89
76	Anomalous losses of deuterium–deuterium fusion products in the Tokamak Fusion Test Reactor*. Physics of Plasmas, 1994, 1, 1469-1478.	0.7	29
77	Model for collisional fast ion diffusion into Tokamak Fusion Test Reactor loss cone. Physics of Plasmas, 1994, 1, 3857-3870.	0.7	12
78	Neoclassical transport coefficients for tokamaks with beanâ€shaped flux surfaces. Physics of Fluids B, 1991, 3, 395-399.	1.7	2
79	Anisotropic distribution function of minority tail ions generated by strong ion yclotron resonance heating. Physics of Fluids B, 1990, 2, 310-317.	1.7	29
80	Effect of impurity particles on the finite-aspect ratio neoclassical ion thermal conductivity in a tokamak. Physics of Fluids, 1986, 29, 3314.	1.4	140
81	Effect of finite aspect ratio on the neoclassical ion thermal conductivity in the banana regime. Physics of Fluids, 1982, 25, 1493.	1.4	204